Available online at www.sciencedirect.com
ScienceDirect
Journal of Power Sources 170 (2007) 85–92
JOURNAL OF POWER SOURCES
www.elsevier.com/locate/jpowsour

A degradation study of Nafion proton exchange membrane of PEM fuel cells

Haolin Tang [a,*], Shen Peikang [b], San Ping Jiang [c], Fang Wang [a], Mu Pan [a]

[a] *State Key Laboratory of Advanced Technology for Materials Synthesis and Processing, Wuhan University of Technology, Wuhan 430070, China*
[b] *State Key Laboratory of Optoelectronic Materials and Technologies, School of Physics and Engineering, Sun Yat-Sen University, Guangzhou 510275, China*
[c] *School of Mechanical and Aerospace Engineering, Nanyang Technological University, 50 Nanyang Avenue, Singapore 639798, Singapore*

Received 3 February 2007; received in revised form 19 March 2007; accepted 29 March 2007
Available online 12 April 2007

Abstract

The durability and degradation behavior of the Nafion NR111 proton exchange membranes (PEMs) is investigated in detail under various mechanical, chemical and polarization conditions. It was found that the fatigue strength or the safety limit of the cyclic stress for Nafion NR111 membrane is ~1.5 MPa that is 1/10 of the tensile strength of the membrane. The cyclic stress and dimensional change (or strain) induced by the water uptake can be substantial and are the main causes for the mechanical degradation and failure of the membrane. For example, in the case of RH cycling of water soaked state to 25% RH state, the cyclic stress of the Nafion membrane was as high as 2.23 MPa and the dimensional change was ~11%. Both FTIR and NMR analysis indicate that the decomposition of the Nafion polymer in the H_2O_2 solution in the presence of trace Fe, Cr and Ni ions started from the ends of the main chain, resulting in the loss of the repeat units and the formation of voids and pinholes in the membrane. The high degradation rate of the membrane at the open circuit voltage most likely results from the attack of H_2O_2 formed between O_2 and H_2 crossovered through the membrane.

Keywords: Fuel cells; Nafion proton exchange membrane; Degradation; Mechanism

1. Introduction

Fuel cells utilizing perfluorosulfonate acid proton exchange membranes (PFSA PEMs) have received much attention because they provide high power density at relatively low operating temperatures. These fuel cells are promising candidates for portable and stationary power sources and for electric vehicle applications. DuPont's Nafion membranes are the state-of-the-art PEMs because of their high proton conductivity and excellent chemical stability. However, enhancement of the stability and durability of the proton exchange membranes are critical to the lifetime and commercial viability of the polymer electrolyte membrane fuel cells (PEMFCs) [1,2]. In order to meet requirements for commercial applications, PEM fuel cells are required to demonstrate durability of about 6000 h under normal operating conditions (e.g. automotive conditions) [3,4]. The stability and integrity of the proton exchange membranes (PEMs) is one of the most crucial factors affect the lifetime of the fuel cells since the PEMs function both as electrolyte and as a separator of the reactant gases.

Durability issue of the proton exchange membrane has attracted extensive attention in recent years [5]. It has been found that the degradation of the fuel cell performance is primarily due to the decay of the membrane-electrode-assembly (MEA) [6–8]. The early failure of the PEMs (<1000 h) is usually contributed to the structural failure of the membranes resulting from the cracking, tearing, puncture, mechanical stresses, inadequate humidification and reactant pressure. The decomposition of the polymer proton exchange membrane associated with the loss of fluoride ion and the decrease of conductivity is also a problem facing the long-term stability of the fuel cell [9,10]. It was shown that the formation of H_2O_2 in the cathodic reaction region can cause the chemical degradation of the membrane [11,12]. The presence of the H_2O_2 had been detected in situ during the fuel

* Corresponding author. Tel.: +86 27 87884448; fax: +86 27 87879468.
E-mail address: tanghaolin2005@yahoo.com.cn (H. Tang).

0378-7753/$ – see front matter © 2007 Elsevier B.V. All rights reserved.
doi:10.1016/j.jpowsour.2007.03.061

cell operating conditions [13]. Pozio and co-workers suggested that the metal ions released from the bipolar plates would accelerate the decay of the proton exchange membrane [14]. The degradation of PEMs may also depend on the operation voltages. It was reported that the degradation rate could be as high as 5.8 mV h^{-1} for the cell operating at open circuit [15].

The long-term operation data obtained from a fuel cell under real operating conditions is very useful for the performance evaluation of a fuel cell in terms of the durability. However, testing of fuel cells for lengthy periods of time is time-consuming and also costly. Thus, ex situ tests were commonly used to study the degradation behaviors [16–18]. For example, using nuclear magnetic resonance (NMR) spectroscopy and mass spectroscopy, common degradation products of Nafion were shown to be produced by in situ (fuel cell operation) and ex situ (Fenton test) testing of membrane [19]. However, the degradation mechanism of the proton exchange membrane is still not clear and not completely understood. In this paper, we investigate various mechanical, chemical and polarization factors affecting the durability and stability of the Nafion polymer electrolyte membrane in detail. The relationship between the membrane breach and the mechanical and chemical effects is discussed.

2. Experimental

2.1. Characterization of the proton exchange membrane

Nafion® NRE 111 membranes, fabricated with chemically stabilized perfluorosulfonic acid/PTFE copolymer, were purchased from DuPont (USA) without further treatment.

Mechanical strength of the Nafion membranes was measured with an electromechanical universal testing machine (WDW-1C) according to a Chinese Standard QB-13022-91. The samples were measured at a strain rate of 50 mm min^{-1}.

The morphologies of the proton exchange membranes were observed by scanning electron microscopy (SEM, JEOL JSM-5610LV, Japan). Cross-section specimens of the proton exchange membranes were prepared by breaking the membrane under liquid nitrogen (77 K). The samples were Au-sputtered under vacuum before the SEM examination.

FTIR spectra of the proton exchange membranes and the solution were recorded on a Nicolet Avatar-370 FTIR spectrometer equipped with a DTGS detector (Nicolet Instrument Corp., USA) with a wavenumber resolution of 4 cm^{-1} in the range of 400–4000 cm^{-1}. The membrane samples were sandwiched between two KBr plates and placed in the cell for measurement. All the samples had standard size of 3.5 cm × 1.5 cm, which covers the whole window to prevent the interference. Liquid samples were mixed with KBr powders and pressed to sheets. The spectra were obtained against the air background spectrum.

^{13}C liquid NMR spectra were obtained at 376 MHz on an Infinity plus 400 spectrometer. All NMR spectra were obtained with proton decoupling. Liquid samples were mixed with 50 v/v% D_2O to keep the solvent (to prevent drift of the magnetic field). Spectra were externally referenced to a water solution of sodium trifluoroacetic acid (singlet assigned to −76.55 ppm). For diluted samples, a Hahn Echo pulse sequence was used to suppress background signals from the probe. Conventional single pulse experiments were used for concentrated samples. The solid ^{13}C NMR experiments were performed at 100 MHz on a Bruker DSX-400 spectrometer. The spectra were acquired on the sample packed in a 2.5 mm rotor with Vespel end-caps, in a 2.5 mm X-H/F double-resonance magic-angle spinning (MAS) probehead at spinning frequencies, ν_r, of 28 or 30 kHz.

The stresses and strain due to the shrinkage caused by the humidification (RH) or temperature change were measured by the Electromechanically universal testing machine with an environmental chamber. The chamber was fitted on the horizontal rail of the machine load frame and had independent T/RH control. The RH control was achieved by slowly circulating a water vapor saturated gas stream at a controlled dew point. In the case of a absolute dry condition (∼0 RH%), the gas stream was dehydrated with anhydrous $CaCl_2$ before entering the clamber. The temperature was controlled by placing electric heating wires inside the chamber and monitored by placing a platinum thermoelectric couple close to the sample. During the test, the samples were cut to spindle shape and two ends of the sample were clamped by the claws of the electromechanical universal testing machine.

2.2. Electrochemical characterization of the proton exchange membranes

The electrochemical characteristics of the proton exchange membranes were measured in a single PEM fuel cell. The fuel cell was fabricated as follows. First, 5 g Pt/C catalysts (40 wt.% Pt/C, Johnson Mathey) were mixed with 50 mL deionized water under vigorous stirring. The 5 wt.% Nafion solution was then added into the mixture and treated by ultrasonics stirring for 30 min and further dispersed in a high-speed homogenizer (20,000 rpm) for 1 h to form a catalyst slurry. The catalyst slurry was sprayed to a PTFE-treated graphitized carbon paper (180 μm, Toray TGP-H-060) to form catalyst electrodes as anode and cathode. Pt catalyst loadings of both electrodes were 0.2 mg Pt cm^{-2} and the dry loadings of Nafion were 0.4 mg cm^{-2}. Anode and cathode with an active area of 25 cm^2 were hot-pressed with the Nafion 111 (28.4 μm thick) membrane to form a membrane-electrode-assembly (MEA). The MEA was mounted in a single cell test fixture with serpentine flow field and a fuel cell clamp (with an active area of 25 cm^2).

The proton conductivity of the membrane was measured by using an impedance analyzer (Autolab PG30/FRA, Eco Chemie, The Netherlands) under the condition of 100% RH and 60 °C. The membrane (2.2 cm × 2.2cm) was sandwiched between two Pt sheets (2 cm × 2 cm) under pressure. One Pt sheet was used as the working electrode and the other as the reference and counter electrodes. EIS was measured in the frequency range of 10 Hz to 100 kHz under the signal amplitude of 10 mV.

The gas permeability or crossover through the Nafion NR111 membranes was assessed by measuring the limiting oxidation current densities of the crossovered H_2 at 80 °C by using the Autolab PG30/FRA. H_2 gas (300 sccm) was fed to the anode side of the cell while N_2 was fed to the cathode. By applying a dynamic potential from 0 to 0.6 V versus the anode (i.e., DHE) at

0.5 mV s^{-1}, the limiting H_2 oxidation current density was measured. The anode side, where hydrogen evolution takes place, served as the counter electrode and the DHE reference electrode.

2.3. Mechanical and chemical tests of the Nafion membranes

A cyclic stress experiment was introduced to investigate the endurance of the proton exchange membrane. The experiments were performed by cutting the Nafion membrane to spindle shape and the two ends of the sample were clamped with the claws of the electromechanical universal testing machine. Then the samples were tested with different stresses cycling every 60 s.

An important accelerating factor for the breach of membrane is the mechanical stress induced by RH cycling and temperature cycling. The RH cycling and temperature cycling experiments were performed by mounting the membrane in a single cell. In the RH cycling experiment, the temperature inside of the single cell was kept at 90 °C. Dry air was fed to the cell for 8 min, followed by humidified air at certain RH level for another 2 min. The RH cycling was achieved by alternatively purging with dry and humidified air gas at a temperature of 90 °C. The limiting oxidation current densities of H_2 diffused through the PEMs were measured every 300 cycles. The catalyst layers in the single cell were replaced every 900 cycles to eliminate the influence of the catalyst layer degradation.

The effect of H_2 and O_2 on the durability of the Nafion NR111 membrane was performed by putting the membrane into bottles under conditions of dry, atmospheric humidity, saturated humidity and 1 mol L^{-1} H_2SO_4. These bottles were fed with 100 sccm H_2 and 100 sccm O_2 respectively. The samples were analyzed after certain period of test.

The effect of metallic impurities in the H_2O_2 solution on chemical stability of the Nafion membrane was tested in a 30 wt.% H_2O_2 solution containing 12.3 ppm Fe, 6.1 ppm Cr, and 5.4 ppm Ni. The metal ions solution was obtained by treating SS316L stainless steel in 0.5 mol L^{-1} nitric acid. SS316L is commonly used as the bipolar plates in PEM fuel cells. The membrane was immersed in the solution and the temperature was kept at 80–90 °C in an oil bath. The solution was analyzed and replaced by fresh solution every 30 min.

The effect of polarization potential at open circuit on the durability of Nafion membrane was also performed in single fuel cells using an Autolab PG30/FRA potentiostat. The open circuit voltage of the cell was measured by feeding H_2 at 300 sccm to the anode and air at 2000 sccm to the cathode. To compare the OCV degradation with pure electrochemical polarization degradation, a voltage of 0.96 V (a value equal to the OCV) was applied to the single cell. In this experiment, the anode (H_2 side) was used as work electrode (WE), the cathode (O_2 side) was used as reference electrode (RE) and counter electrode (CE). With N_2/O_2 and H_2/N_2 as anode/cathode gases supply, respectively, the voltage of 0.96 V was applied to the WE (anode) to simulate the polarization of the fuel cell at OCV. In every 500 min, the polarization was interrupted and the OCV of the cell was measured by switching the anode/cathode gases to H_2/O_2.

3. Results and discussion

3.1. Mechanical stability of the Nafion NR111 membrane

In order to investigate the fatigue strength of the Nafion membrane, a cyclic stress experiment was conducted and the results are shown in Fig. 1. It is obvious that the PEM was very stable and almost had no dimensional change under the cyclic stress equal to or less than 1.5 MPa. However, the dimension of the membrane changed significantly and the microstructure breakdown appeared on the surface when the cyclic stress was over 3.0 MPa. After 1000 cycles at a cyclic stress of 4.0 MPa, the membrane was elongated and the membrane became thinner. With the cyclic stress further increased to 6.5 MPa, many cracks appeared on the surface of the Nafion membrane, indicating the rupture of the membrane microstructures. Considering that the tensile strength of Nafion 111 membrane is about 23–28 MPa [20], the results of the cyclic stress tests clearly indicate that the PEMs could be destroyed under much lower stress under conditions of fatigue stress than that of static tensile stress. For the fatigue stress condition, the Nafion PEM could only survive the cyclic stress lower than or equal to 1.5 MPa. This implies that the fatigue strength of the Nafion NR111 membrane is about 1/10 of the tensile strength of the membrane.

It is well known that the cyclic stress in the fuel cell can be generated from the gas and water, which passes through the gas diffusion layers and may give an impulsion force vertically to the membrane. However, the impulsion pressure generated from gas and water fluid would be no more than 1 MPa based on the air compressor supplied fuel cell stacks [21,22]. Hence, the impulsion stress generated by the gas and water fluid to the cell may not be high enough to cause serious damage to the PEMs.

The stress in the membrane of a fuel cell can also be resulted from the shrinkage and consequently the dimensional change of the membrane, especially the dimensional change in-plane direction since the four sides of the membrane are fixed in the fuel cell. In addition to the excessive stress formed during the

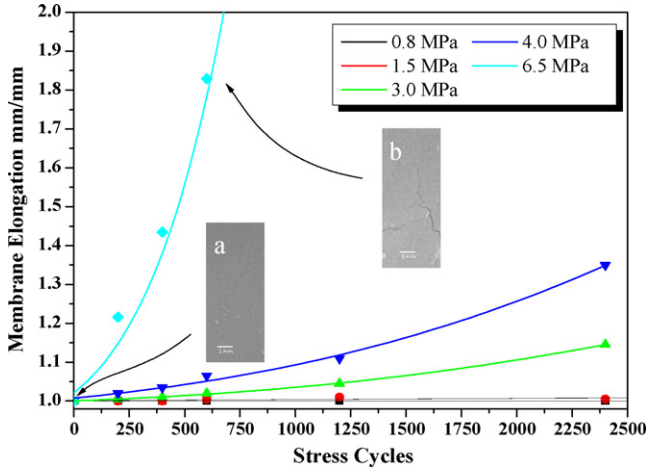

Fig. 1. Elongation of Nafion 111 membrane in the stress direction as a function of various fatigue stress cycles. The inset pictures are the surface SEM micrographs of (a) as-received Nafion 211 membrane, (b) the Nafion 211 membrane after 540 cycles under stress switched between 0 and 6.5 MPa.

cell assembly, the dimensional change may also be induced by the change of the cell temperature and water uptake of the membrane during the fuel cell operation. Fig. 2 shows the stress and dimensional change caused by the shrinkage under various RH cycling at 25 °C. In the case of RH cycling from water soaked state to 25% RH at 25 °C, the samples with a spindle shape soaked in water were clamped by the claws of test machine at temperature of 25 °C. The humidity in the chamber was slowly reduced from the initial water soaked state to 25% RH. The shrinkage stress induced by the RH cycling from water soaked state to 25% RH at 25 °C was quite high, reaching a maximum value of 2.23 MPa and stable at 2.1 MPa at the end of the test. This stress is higher than that of the safety limit of the fatigue stress of 1.5 MPa for Nafion NR111 membrane as shown in Fig. 1. However, the shrinkage stress of the PEM decreased significantly with the decrease of the initial RH level (Fig. 2a). The shrinkage stress of the membrane with initial RH state of 100% RH and 60% RH was 1.32 and 0.48 MPa, respectively.

The dimensional change induced by the RH cycling can be quite large. For example, for the RH cycling from the water soaked state to 25% RH state, the dimensional change (or strain) is ~11% (Fig. 2b). Nevertheless, similar to the shrinkage stress, the dimensional change decreases with the decrease in the initial RH level. It is obvious that the shrinkage stress increases with the increase of the initial RH level, which is consistent with the trend of the membrane dimensional change induced by swelling. This indicates that the shrinkage stress of the membrane due to the RH cycling is induced by the dimensional change associated with the swelling of the membrane.

An additional experiment on the shrinkage stress was performed by changing the temperature between 80 and 25 °C under absolute dry condition (~0% RH). The value of the shrinkage stress was about 0.14 MPa (see Fig. 2a), which is much smaller than that of the stress under RH cycling tests. This result revealed that the stress induced by temperature cycling is very low and would be not responsible for the mechanical breach. However, in the fuel cell operating condition, the gas is generally humidified and the water produced also humidifies the membrane of the cell. Therefore, it is necessary to investigate the effect of temperature cycling on the stress behavior of the membrane under the humidified condition. In this test, inlet gas was humidified at 80 °C. As shown in Fig. 2a, a large shrinkage stress of ~1.76 MPa was generated under the same temperature cycling conditions. This result showed that the membrane degradation was increased significantly when the membrane was subject to temperature cycling and humidity conditions simultaneously.

Fig. 3 shows the limiting oxidation current densities of the crossovered H_2 of the membranes under various RH cycling conditions. At the early stage of the RH cycling experiments, the H_2 crossover current density was in the range 1–2 mA cm^{-2} and the change in the H_2 crossover current density is negligible. When the membrane was cycled between the water soaked state and 25% RH state every 10 min, the significant increase in the H_2 crossover current density started after 3000 cycles. After 4000 cycles, the increase in the H_2 crossover is exponential, indicating the mechanical breach and failure of the membrane. However, the H_2 crossover was almost constant and the value was less than 2 mA cm^{-2} for over 7000 cycles if the initial RH level of the gas was 100% RH or lower at 25 °C. This result is consistent with the cyclic stress and the shrinkage stress experiments as the membrane is stable if the fatigue stress is less than 1.5 MPa. As shown

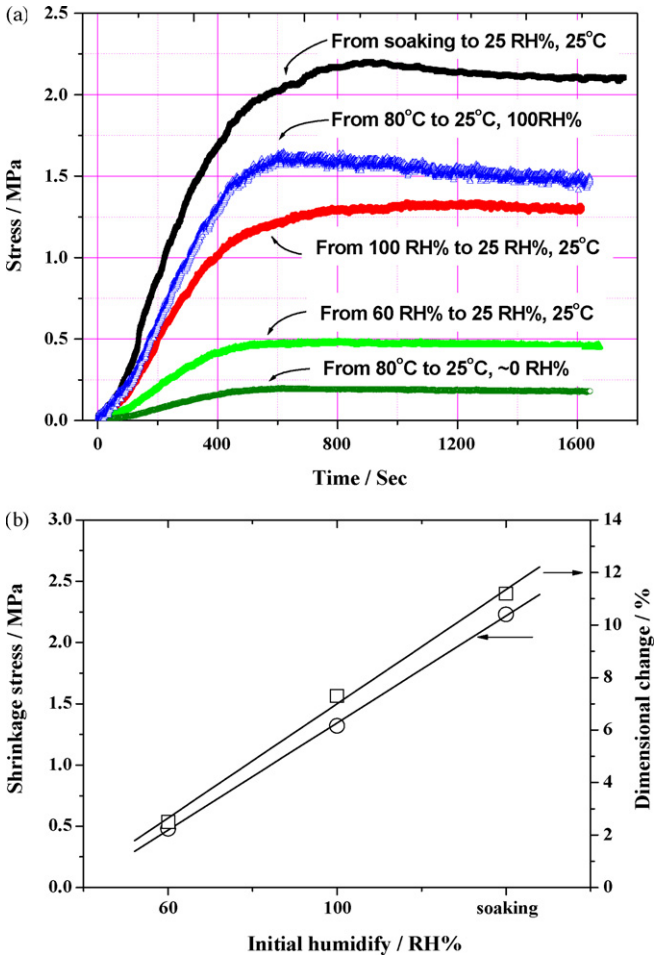

Fig. 2. (a) Shrinkage stress of Nafion membrane at 25 °C under different initial humidities. (b) The shrinkage stress and dimensional change of the Nafion membrane as a function of humidity.

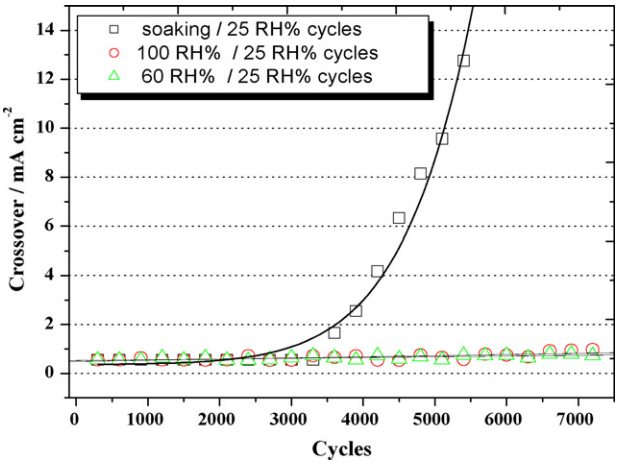

Fig. 3. H_2 crossover current densities of Nafion membranes as a function of the dry/wet cycles.

in Fig. 2, the shrinkage stress of the membrane induced by the RH cycling from the water soaked state to 25% RH and from 100% RH to 25% RH at 25 °C were 2.23 and 1.32 MPa, respectively.

3.2. Chemical stability and decomposition of the proton exchange membrane

Membrane electrode assembly with proton exchange membrane and catalyst layer is the electrochemical reaction region of the fuel cell. Except H_2O, H_2 or O_2, the intermediate product of H_2O_2 is found during the operation in a fuel cell. Due to the acidic and humidity environment in fuel cells, some metal ions form stainless steel may be released. Hence the presence of H_2, O_2, H_2O_2 and metal ions should be taken into account for the decay of proton exchange membrane [23].

In order to investigate the potential influence of H_2 or O_2 on the membrane chemical stability, an experiment on the proton exchange membrane exposed in pure H_2 or O_2 atmosphere was introduced in this research. The conditions that would exist in the fuel cell, such as absolute dry, atmospheric humidity, saturated-humidity, acid were considered. The reflective FTIR spectra of the Nafion 111 membrane are shown in Fig. 4. As reported elsewhere [24], the spectrum of Nafion membrane exposed for various periods of time shows main peaks at ~1200, ~1100, ~1060 and ~980 cm^{-1}, which were identified as CF_2 asymmetric stretching, CF_2 symmetric stretching, S–O symmetric stretching and symmetric C–O–C stretching, respectively. With a long-term exposure to H_2 or O_2 for 1000 h, the main peaks of the spectrum were hardly changed, indicating the chemical stability of Nafion membrane in the H_2 and O_2 environment. The proton conductivity and tensile strength of the Nafion membrane also did not change significantly. The chemical and physical properties of the Nafion membranes are summarized in Table 1.

The O_2 reduction reaction can occur via a 4-electron or 2-electron pathway. In the case of acidic electrolyte, the 2-electron reaction pathway generally occurs with the production of H_2O_2 intermediate species [25]. In the presence of transition metal ions, H_2O_2 will subsequently convert to •OH radical [26]. In order to investigate the effect of H_2O_2/metal ion solution on the stability of the Nafion membrane, an accelerating experiment

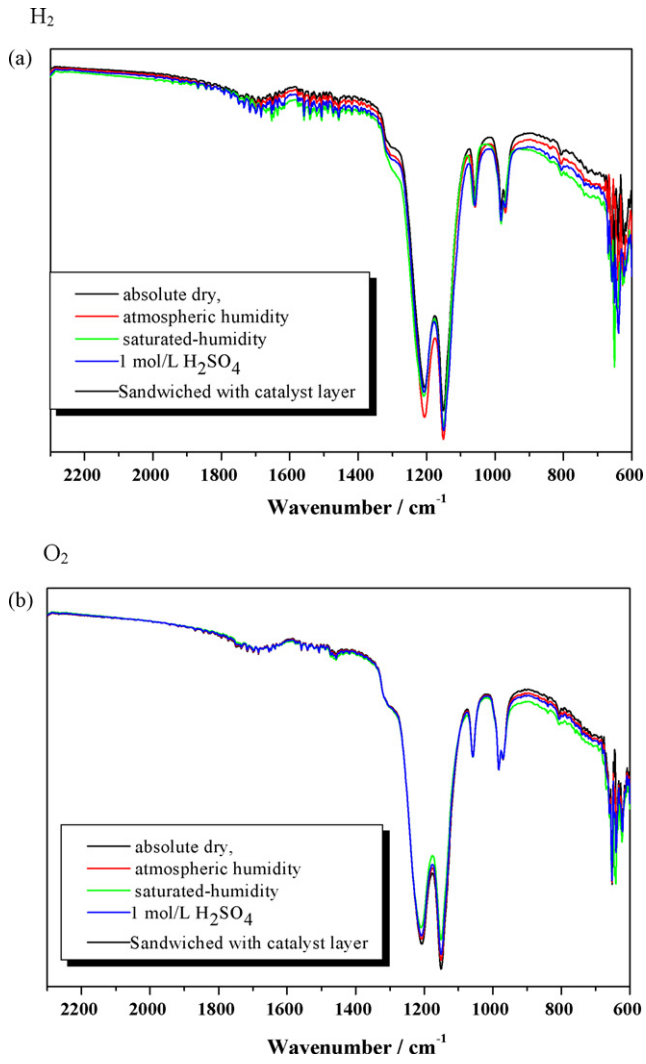

Fig. 4. The reflective FTIR spectra of the Nafion membrane in (a) 100 sccm of H_2 and (b) 100 sccm of O_2 at the condition of dry, atmospheric humidity, saturated humidity and 1 mol L^{-1} H_2SO_4.

Table 1
Chemical and physical properties of Nafion membranes exposed in H_2 or O_2 for 1000 h

	Thickness (μm)	EW value	Conductivity (S cm^{-1})	Tensile strength (MPa)
Original Nafion111	25.4 ± 0.1	1058 ± 50	0.11 ± 0.01	22.3 ± 0.5
1000 h H_2				
Absolute dry	25.1 ± 0.1	1034 ± 50	0.10 ± 0.01	23.6 ± 0.5
Atmosphere humidity	24.8 ± 0.1	1046 ± 50	0.11 ± 0.01	22.1 ± 0.5
100% RH	25.2 ± 0.1	1065 ± 50	0.11 ± 0.01	21.5 ± 0.5
Acidic condition	24.3 ± 0.1	1073 ± 50	0.12 ± 0.01	20.9 ± 0.5
With Fe^{2+}	22.4 ± 0.1	1037 ± 50	0.10 ± 0.01	21.6 ± 0.5
1000 h O_2				
Absolute dry	25.2 ± 0.1	1084 ± 50	0.10 ± 0.01	23.3 ± 0.5
Atmosphere humidity	24.3 ± 0.1	1058 ± 50	0.11 ± 0.01	22.5 ± 0.5
100% RH	24.2 ± 0.1	1063 ± 50	0.11 ± 0.01	21.6 ± 0.5
Acidic condition	23.9 ± 0.1	1042 ± 50	0.10 ± 0.01	21.7 ± 0.5
With Fe^{2+}	23.4 ± 0.1	1067 ± 50	0.10 ± 0.01	20.8 ± 0.5

was performed by treating the membrane in a solution containing 30 wt.% H_2O_2 and metal ions of 12.3 ppm Fe, 6.1 ppm Cr, and 5.4 ppm Ni. The solutions collected at 48, 72 and 96 h were analyzed. Fig. 5a shows the FTIR spectra of the polymer fragments collected from the solution. The stretching peaks that appear at ~1700 and 930 cm^{-1} can be attributed to C=O stretching and S=O stretching bands, which are possibly due to the existence of $–SO_3^-$ and –COOH groups in the decomposed fragments. The C-F symmetric stretching peaks at 1200 and 510 cm^{-1} clearly revealed the existence of C–F bands and the F^- ions released from the Nafion polymer. By using the Atom Adsorption Spectrum, the F^- releasing rate, which is corresponding to the decomposition of the Nafion membrane, was measured and is illustrated as the inset of Fig. 5a. The F^- releasing rate (FER) was about 0.15 mg h^{-1}, corresponding to 0.036 wt.% of F was released from the membrane per hour (the sample was 10 cm × 10 cm, 28.4 μm thick and 2.94 g cm^{-3} in density. F content in the membrane was about 51 wt.%). The chemical structure of the decomposed fragments was further identified by using the 96 h treated solution for ^{13}C NMR analysis. As shown in Fig. 5b, there were four types of C in the solution, which was C=O at 168.0, CF at 68.5, CF_2 at 63.0 and CF_3 at 61.5. Compared to the Nafion structure (the inset in Fig. 5b), only the side chain of the Nafion polymer have these bands. Therefore, it is reasonable to conclude that the decomposed fragments are the side chains of the Nafion polymer. The existence of the C–O–C bands and S=O bands further provides the evidence (Fig. 5a). Relatively speaking, the C–C bands are very stable and the existence of the F can strongly protect the bands due to the small ion diameter and low electronegativity. As the Nafion polymer is produced by the copolymerization of tetrafluoroethylene (TFE) and perfluorovinyl ether monomers and several volatiles would exist in the resulting polymers including unstable end groups such as –COF, COOH [27,28]. This process possibly introduces many of C=O bands into the polymer ends, which are not stable in the •OH-containing solution.

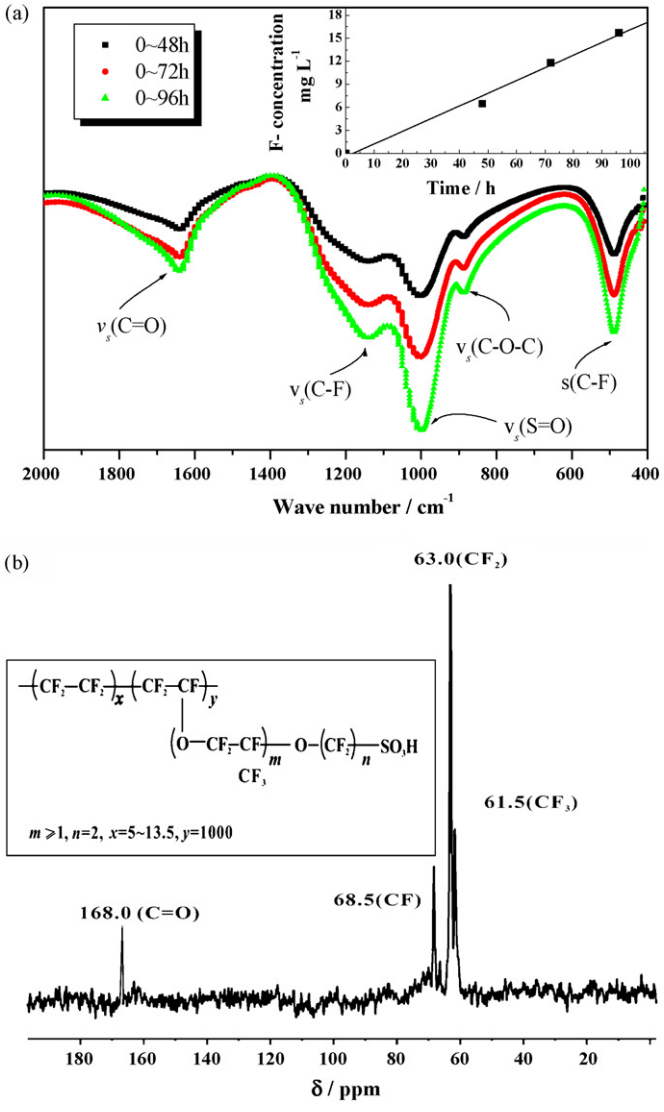

Fig. 5. (a) FTIR spectra and (b) ^{13}C NMR spectrum of the H_2O_2/metal ions after the Nafion polymer was immersed in the solution for various period of time. The inset of (a) is the decomposed F content and the inset of (b) is the chemical structure of Nafion polymer.

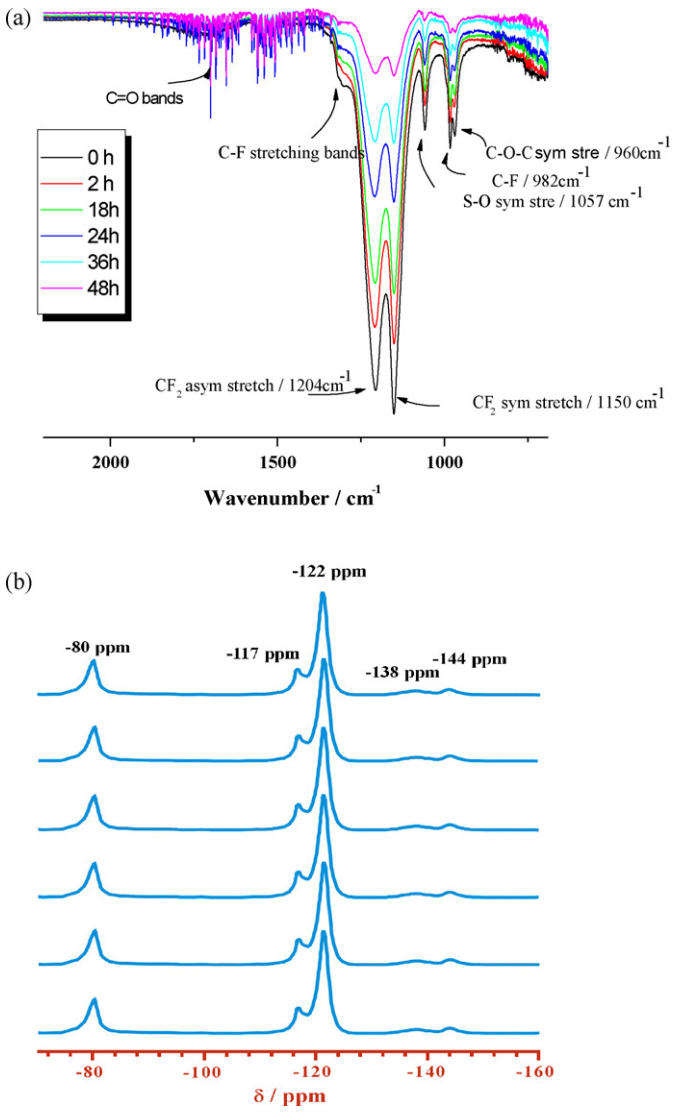

Fig. 6. (a) Reflective FTIR spectra and (b) solid ^{13}C NMR spectrum of the Nafion membranes after treating in H_2O_2/metal ions for various period of time.

The structure change of the Nafion membranes during the H_2O_2/metal ions treatment was also investigated. Fig. 6a shows the reflective FTIR spectra of the Nafion membrane as a function of the soaking time in the solution. There is a synchronous decrease in the relative intensities of all the CF_2 asymmetric stretching, CF_2 symmetric stretching, S–O symmetric stretching and symmetric C–O–C stretching with the increase of the soaking time. However, the changes of the relative intensities of all groups were not observed in the NMR spectra (Fig. 6b). Considering that the FTIR is an area reflection, while the NMR is a statistical analysis of the polymer contact powder, the contrast of the reflectance-FTIR and the NMR reveal that the degradation of the PEMs comes from the decomposition of the repeating units in the main chain of the polymer.

The surface SEM morphologic examination showed that the chemical degradation introduced many small bubbles on the surface (Fig. 7a) and pores in the cross-section area (Fig. 7b) of the Nafion membrane. The small bubbles gradually became pinholes during the chemical decay process. Considering that the membrane was stress-free during the test, the appearance of the bubbles was most likely resulted from the decomposition of the polymer repeating units. With the increase in the decomposition of the repeating units the little voids appeared in the membrane due to the loss of the repeating units. The little voids and the resulted pinholes will result in the substantial increase in the gas crossover.

3.3. Effect of polarization on the degradation of the Nafion membranes

Fig. 8 is the open circuit potential of the cell measured under various polarization conditions at 25 °C. In the case of H_2/O_2 as anode and cathode gases, the open circuit voltage, V_{oc}, decreased significantly from initial 0.96 to ~0.64 V after 3000 min at open circuit condition. The V_{oc} decreasing rate was about 0.11 mV min^{-1}. In order to identify the origin of the degradation, a polarization potential was applied to a PEM fuel cell under different anode and cathode gases. During the test, a voltage of 0.96 V was applied to the anode (H_2) to simulate the polarization of the fuel cell at OCV. The polarization stopped every 500 min and the H_2/N_2 was supplied to the fuel cell to measure the change of the OCV and the H_2 crossover. As shown in the Fig. 8, the OCV was constant under N_2/O_2 and H_2/N_2 anode and cathode gases, suggesting that the membrane-electrode-

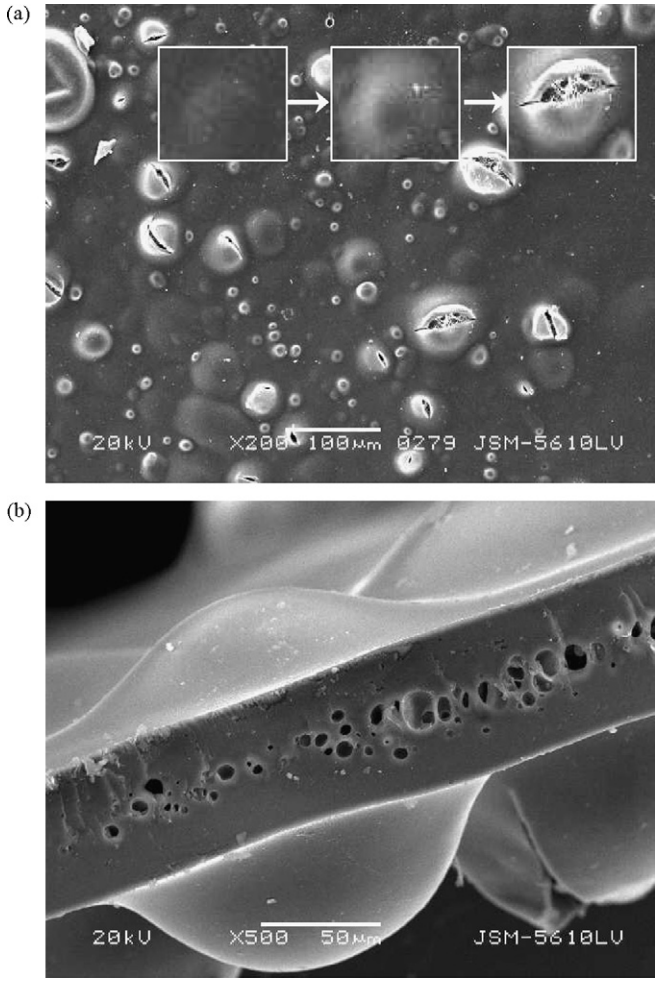

Fig. 7. (a) Surface and (b) cross-section SEM micrographs of the Nafion membranes treating in H_2O_2/metal ions containing solution for 48 h.

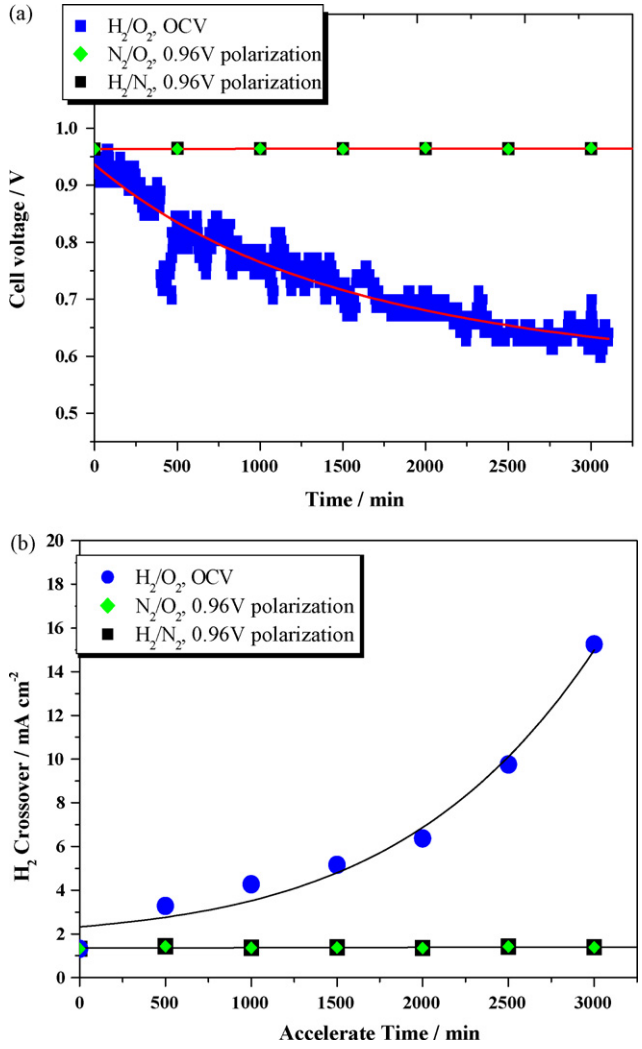

Fig. 8. (a) The cell open circuit voltage and (b) H_2 crossover of a fuel cell polarized at various conditions.

assembly materials, including the proton exchange membrane, are very stable if only voltage polarization is applied. The results in this study also suggests that the degradation at the open circuit is not due to polarization potential or the presence of the H_2 or O_2, but most likely due to the presence of H_2 and O_2 at the anode and cathode simultaneously, leading to the formation of H_2O_2 intermediate species as the result of the H_2 crossover from the anode. The two pathways of oxygen reduction have been quantitatively studied using rotating-ring disk electrodes (RRDE) [29]. The yield of H_2O_2 increases with the decrease in disk potential to the maximum in the potential range of H_2 adsorption, i.e., near the anode potential in an operating fuel cell. In a fuel cell at the presence of H_2/O_2, the H_2 can permeate to cathode through Nafion membrane (indicated by the H_2 crossover current of 1–2 mA cm^{-2}). At the open circuit voltage condition, the reduction of O_2 with the permeated H_2 is preceded via the pathway of forming H_2O_2, causing the chemical degradation membrane, indicated by the significant increase of the H_2 crossover current (Fig. 8b).

4. Conclusions

The degradation behavior of Nafion NR111 membrane was studied under various mechanical, chemical and polarization conditions. The safety limit of the cyclic or fatigue strength of the Nafion NR111 membrane was 1.5 MPa that is 1/10 of the tensile strength of the membrane. The cyclic stress and dimensional change (or strain) induced by the RH cycling can be substantial. For example, in the case of RH cycling of water soaked state to 25% RH state, the cyclic stress of the Nafion membrane was as high as 2.23 MPa and the dimensional change was ∼11%. Such cyclic stress induced by the RH cycling can lead to the rapid mechanical breach and failure, indicated by the substantial gas crossover after 3000 cycles in the case of water soaked state/25% RH cycling test. It is concluded that the shrinkage stress generated by the water-uptake is responsible for the mechanical decay of the Nafion PEMs.

The Nafion membranes were stable in the separated H_2 and O_2 atmosphere at various conditions of dry, atmospheric humidity, saturated humidity and acidic solution. The decomposed fragments were found in the H_2O_2 solution in the presence of Fe, Cr and Ni ions. Both FTIR and NMR analysis indicate that the decomposition of the Nafion polymer started from the ends of the main chain, resulting in the loss of the repeat units. The voids and pinholes appeared in the proton exchange membrane with the increase in the repeat unit loss and caused the membrane hazard of gas crossover. The high degradation rate of the membrane at the open circuit voltage most likely results from the attack of H_2O_2 formed at the potential close to the H_2 adsorption potential.

Acknowledgements

The author would like to thank WUT New Energy Co. Ltd. for the financial and equipment support. This work was also supported by Program for Changjiang Scholars and Innovative Research Team in University (PCSIRT, no. IRT0547).

References

[1] C. Iojoiu, F. Chabert, M. Marèchal, N.El. Kissi, J. Power Sources 153 (2006) 198.
[2] U. Beuschern, Y.S. Cleghorn, W. Johnson, Int. J. Energy Res. 29 (2005) 1103.
[3] U.S. Department of Energy, Multi-Year Research, Development and Demonstration Plan: Planned program activities for 2003–2010, pp. 3.5-1.
[4] U.S. Department of Energy, Draft Funding Opportunity Announcement Research and Development of Polymer Electrolyte Membrane (PEM) Fuel Cells for the Hydrogen Economy, pp. 4.
[5] A. Collier, H. Wang, X.Z. Yuan, J. Zhang, D.P. Wilkinson, Int. J. Hydrogen Energy 31 (2006) 1838.
[6] Z. Luo, D. Li, H. Tang, M. Pan, R. Yuan, Int. J. Hydrogen Energy 31 (2006) 1831.
[7] S. Cleghorn, D. Mayfield, D. Moore, J. Moore, G. Rusch, T. Sherman, N. Sisofo, U. Beuscher, J. Power Sources 158 (2006) 446.
[8] W.M. Chen, G.Q. Sun, J.S. Guo, X.S. Zhao, S.Y. Yan, J. Tian, S.H. Tang, Z.H. Zhou, Q. Xin, Electrochim. Acta 51 (2006) 2391.
[9] O. Vishal Mittal, H. Kunz, J. Fenton, J. Electrochem. Soc. 153 (2006) A1755.
[10] W. Mèrida, D. Harrington, J. LeCanut, G. McLeand, J. Power Sources 161 (2006) 264.
[11] M. Aoki, H. Uchida, M. Watanabe, Electrochem. Commun. 8 (2006) 1509.
[12] J. Qiao, M. Saito, K. Hayamizu, T. Okadaz, J. Electrochem. Soc. 153 (2006) A967.
[13] V. Mittal, H. Kunz, J. Fentonb, Electrochem. Solid-State Lett. 9 (2006) A299.
[14] A. Pozio, R.F. Silva, M. De Francesco, L. Giorgi, Electrochim. Acta 48 (2003) 1543.
[15] K. Teranishi, K. Kawata, S. Tsushima, S. Hirai, Electrochem. Solid-State Lett. 9 (2006) A475.
[16] A. Laconti, M. Hamdan, R. Mcdonald, Handbook of Fuel Cell, vol. 3, John Wiley and Sons Ltd., Chichester, England, 2003, pp. 647.
[17] X. Huang, R. Solasi, Y. Zou, M. Feshler, K. Reifsnider, D. Condit, S. Burlatsky, T. Madden, J. Polym. Sci. B 44 (2006) 2346.
[18] D.A. Stevens, J.R. Dahn, Carbon 43 (2005) 179.
[19] J. Healy, C. Hayden, T. Xie, K. Olson, R. Waldo, M. Brundage, H. Gasteiger, J. Abbott, Fuel Cells 5 (2005) 302.
[20] Du Pont report, DuPont™ Nafion® PFSA Membranes: NRE111 and NRE212, http://www.dupont.com/fuelcells/pdf/dfc201.pdf.
[21] C. Bao, M.G. Ouyang, B.L. Yi, J. Hydrogen Energy 31 (2006) 1879.
[22] S. Pisching, O. Lang, Handbook of Fuel Cell, vol. 4, John Wiley and Sons Ltd., Chichester, England, 2003, pp. 728.
[23] J.R. Yu, T. Matsuura, Y. Yoshikawa, M.N. Islam, M. Hori, Phys. Chem. Chem. Phys. 7 (2005) 373.
[24] Z. Liang, W. Chen, J. Liu, S. Wang, Z. Zhou, W. Li, G. Sun, Q. Xin, J. Membr. Sci. 233 (2004) 39.
[25] P.C. Foller, R.T. Bombard, J. Appl. Electrochem. 25 (1995) 163.
[26] C. Mansano-Weiss, H. Cohen, D. Meyerstein, J. Inorg. Biochem. 91 (2002) 199.
[27] R.A. Morgan, W.H. Sloan, Extrusion finishing of perfluorinated copolymers, U.S. Patent 4,626,587.
[28] M. Doyle, G. Rajendran, Perfluorinated Membranes, Handbook of Fuel Cell, vol. 3, John Wiley and Sons Ltd., Chichester, England, 2003, pp. 351.
[29] U.A. Paulus, T.J. Schmidt, H.A. Gasteiger, R.J. Behm, J. Electroanal. Chem. 495 (2001) 134.